

RAPID ESTIMATION OF VOLUMETRIC GROUNDWATER RECHARGE IN THE VADOSE ZONE VIA GROUND PENETRATING RADAR

Alexander Ross Costall*
Curtin University
26 Dick Perry Avenue, W.A
Alex.costall@curtin.edu.au

Brett Harris
Curtin University
26 Dick Perry Avenue, W.A
b.harris@curtin.edu.au

*presenting author asterisked

SUMMARY

Saturation in the vadose zone is known to reduce the ground penetrating radar (GPR) electromagnetic wave velocities. We examine the impact of increased water content in highly-permeable beach and dune systems on GPR velocities along coastal margin of Perth, Western Australia. We acquire repeat GPR transects in May and August before and after annual high rainfall periods. The assumption of exceedingly flat water table reflector permits us to estimate change in GPR velocity at successive dates. This change in velocity can be translated to an estimated change in water saturation via the Topp relationship which is an empirical mapping of water saturation to dielectric permittivity.

Key words: Ground Penetrating Radar, Water-Table, Vadose-zone recharge

INTRODUCTION

Ground Penetrating Radar (GPR) is an effective tool for shallow high-resolution geophysical investigation. The speed and simplicity of acquisition lends itself to rapid detection and evaluation of subsurface features. Variations in relative dielectric permittivity below the ground cause high-frequency electromagnetic waves to be reflected from layers with sufficient electrical impedance contrast.

The vadose zone in semi-arid quartz or limestone coastal environments is usually highly resistive and internal structure of beach and dune sediments can be exceedingly well resolved by GPR. However it is the high-contrast boundary at the water table that often provides the strongest GPR reflection. Other reflections in the vadose zone are typically the result of grain-size or mineralogy changes, including high concentrations of heavy minerals (exceeding 2.9 g. cm^{-3}) such as those formed from storm-lag deposits (Buynevich, Jol, & FitzGerald, 2009). Changes in depositional environments are identifiable in GPR.

Examples where GPR has been applied include stratigraphic mapping (Davis & Annan, 1989), soil-water content definition (Huisman, Hubbard, Redman, & Annan, 2003), porosity estimation (Bradford, Clement, & Barrash, 2009; Turesson, 2006), and water table/vadose zone depth evaluation (Elmar Strobach, 2013; Elmar Strobach, D. Harris, Christian Dupuis, W. Kepic, & W. Martin, 2010). The dominant factors controlling the depth of investigation for GPR are antennae bandwidth, and ground conductivity. Higher-frequency antennas tend to be able to resolve close spaced layers at the expense of depth penetration. Highly conductive media, such as clays and saline water, will attenuate the GPR signal and dramatically reducing the investigation depth. The velocity of an electromagnetic wave in a medium is (BurVal Working Group, Kirsch, Rumpel, Scheer, & Wiederhold, 2006);

$$v = \frac{c}{\sqrt{\epsilon_r \mu_r \frac{1 + \sqrt{1 + \left(\frac{\sigma}{\omega \epsilon}\right)^2}}{2}}} \quad (1)$$

In the case of low-loss materials such as clean, dry, quartz sands, equation (1) reduces to

$$v = \frac{c}{\sqrt{\epsilon_r}} \quad (2)$$

Changes in surface elevation such as dunes are significant for imaging and analysis of GPR data. Sand dunes in Perth can extend to 40 metres above-sea-level (ASL) in the northern-most suburbs such that depth to the water table will be outside the range of most shielded GPR systems. We target accuracy of less than 10cm which can be achieved with real-time kinematic (RTK) global-position-systems (GPS). This is necessary for precise mapping of the water table GPR reflector.

METHOD AND RESULTS

The velocity of the GPR electromagnetic pulse is related to electrical permittivity. Water has a high relative electrical permittivity (e.g. 80) and thus even a small change in water saturations can significantly impact GPR velocity in the vadose zone (Topp, Davis, & Annan, 1980). The Topp relationship (Topp et al., 1980) (equations 3, and 4) shown in Figure Error! No text of specified style in document..1, is an empirically derived relationship between dielectric permittivity and water saturation. The empirical nature of the relationship tends to break down at very low (i.e. < 5%) and very high (i.e. > 40%) water saturation, resulting in a wider margin of error at these extremes (Elmar Strobach, 2013).

$$\epsilon'_{e,r} = 3.03 + 0.3\theta_v + 146 \theta_v^2 - 76.7\theta_v^3 \tag{3}$$

$$\theta_v = -5.3 * 10^{-2} + 2.92 * 10^{-2} \epsilon_{e,r} - 5.5 * 10^{-4} \epsilon_{e,r}^2 + 4.3 * 10^{-6} \epsilon_{e,r}^3 \tag{4}$$

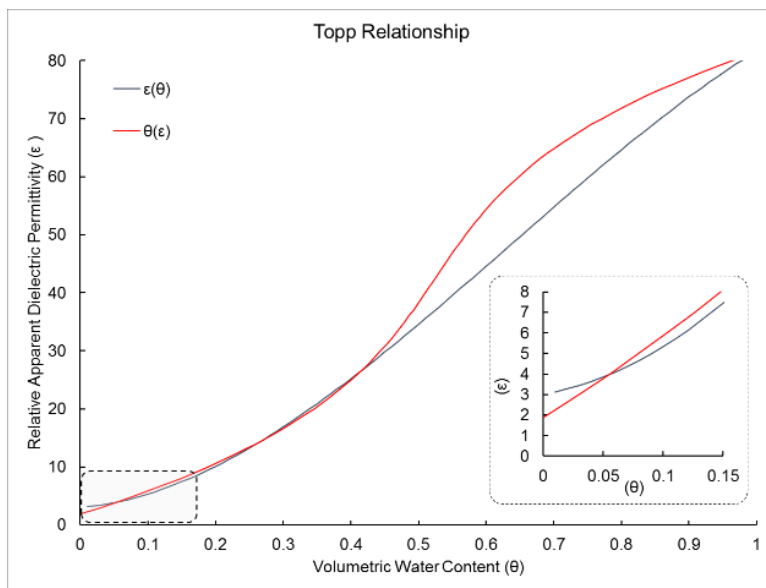


Figure Error! No text of specified style in document..1: Graph of the ‘Topp relationship’ (Topp et al., 1980) relating the volumetric water content and dielectric permittivity of a medium. Note the difference between the forward and reverse relationships at lower volumetric water contents, prominent at high (i.e. > 40%) volumetric water content. Graph shown from equations 3 and 4 (Topp et al., 1980).

We refer to water in the vadose zone (i.e. between the ground surface and phreatic water table), as ‘volumetric unsaturated zone water content’ or simply volumetric water content. Rate of rainfall infiltration through the unsaturated zone will depend on rainfall, evapotranspiration, and unsaturated hydraulics of the sediments. Water saturation will affect the relative dielectric permittivity (ε) as shown by the Topp relationship (Figure Error! No text of specified style in document..1), and reduce the GPR pulse velocity, e.g. Figure Error! No text of specified style in document..2. Changes in water saturation can be estimated from repeat GPR surveys.

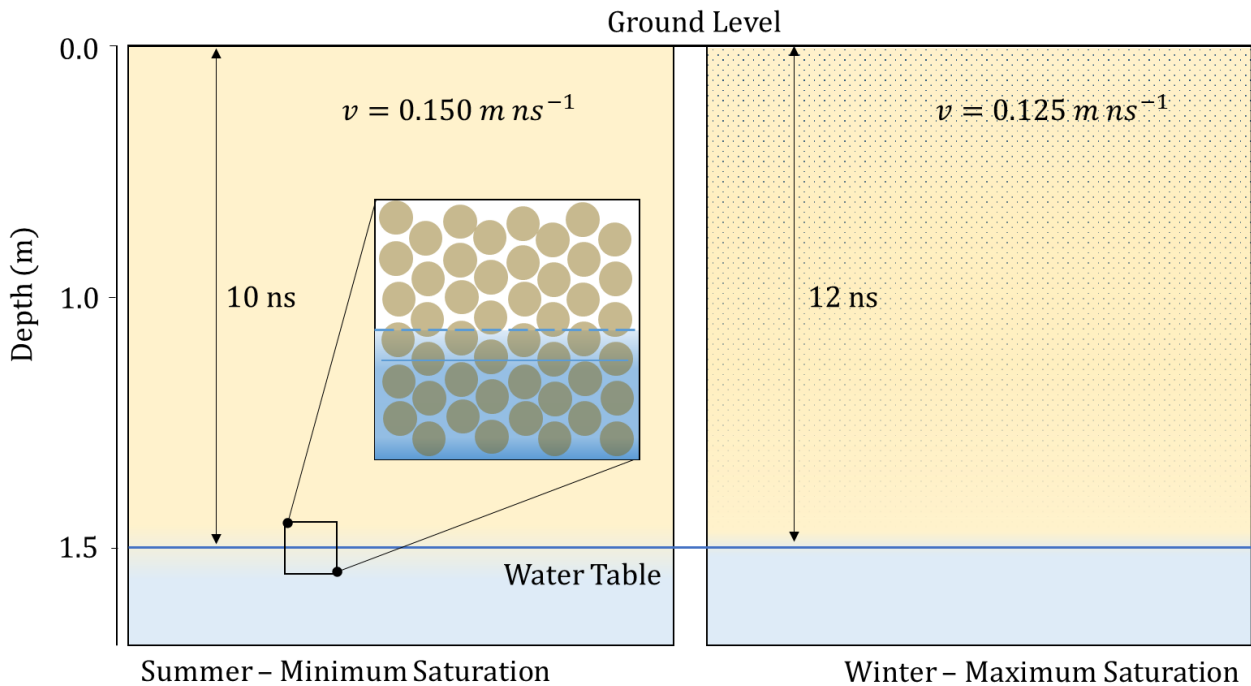


Figure Error! No text of specified style in document..2: Representation of the velocity reduction effect of water saturation, as inferred from the Topp relationship. An increase in water content will increase the relative apparent dielectric permittivity and reducing the GPR wave velocity. This schematic shows a highly permeable media, such as a coarse beach sand. For high permeability sediments, the impact of rainfall recharge on the water table will be negligible near to the ocean (e.g. a known head boundary dictated by tidal forcing). The capillary fringe in a coarse sand environment is also expected to be negligible.

Data collected by a local monitoring station at Swanbourne suggests that rainfall for the year 2014 was unusually low, at 581.2 mm for the entire year. This is considerably lower than both the historical average since 1993 (when these records began), and the preceding two years. E. Strobach, Harris, Dupuis, and Kopic (2014) suggests rainfall at several location in the Bassendean Sand of the Gngangara mound aquifer system may infiltrate at rates of close to 2 metres per 3 month period. It's possible that infiltration rates through the sands at the city beach site could be similar or faster than of the Bassendean Sands.

Worldwide study locations suggest infiltration rates of 34.5% for permeable skeletal soil of low water-holding capacity (Allison & Hughes, 1978), while Stephens and Knowlton (1986) suggests up to 20% for coarse-grained sands with very small percentage of silt and clay. Local infiltration studies from Banksia woodland vegetation in the Gngangara mound suggest a value of 194 mm/year for approximately 800 mm of rainfall, i.e. 24% (Sharma, Farrington, & Fernie, 1983), which agree with geophysical infiltration studies by E. Strobach et al. (2014).

We make the assumption near flat water table at mean sea level, over the length of the GPR transect. A nearby well suggests a water-table gradient of 1.07 mm/m in October and 0.61 mm/m in May. These numbers suggest that the maximum rise in the water table from the ocean to the end of the GPR transect is less 18 cm in May, and less than 30 cm in August.

Four transects, shown in Figure **Error! No text of specified style in document..3**, were collected on the 2nd May 2014 and then again on the 8th August 2014 using the common offset radar method. These transects were measured with the Mala ProEx GPR system in combination with a 250 MHz towed sled-style shielded antenna. Radar measurements were made ten times a second (10 Hz), and synchronised with a Thales Z-Max real-time kinematic (RTK) global positioning system (GPS) for precise elevation control. Each trace is stacked four times to improve signal-to-noise ratio. Processing steps undertaken are common between vintages (i.e. May and August transects), including de-wow, static correction, subtracting average, band-pass filtering and an energy-decay gain function.



Figure Error! No text of specified style in document..3: Location and orientation of the ground penetrating radar (GPR) transects featured in this paper. Shallow geology is described predominantly Tamala Limestone and Safety Bay sands. Total perpendicular length from the coastline is approximately 300 m.

After diffraction velocity analysis of the sections, a depth-conversion velocity of 0.145 m/ns is found to be appropriate. This value satisfies the flat water-table reflection assumption for May. Velocities ranging from 0.1 to 0.2 m/ns were tested however 0.145 m/ns was optimal (i.e. provided a flat water table reflector), and agreed with the majority of diffractions. Butler (2005) suggests 0.15 m/ns is reasonable for dry sands, in agreement with our finding.

Figure Error! **No text of specified style in document..4** shows that using a velocities of 0.145 m/ns for time to depth conversion of the August GPR data fails to flatten the water table reflector. The August water-table reflection is clearly bowed in the centre of the profile. The geometry of the reflector at 0.145m/ns may be due to lithological changes, such as lower-porosity limestone, or finer sands.

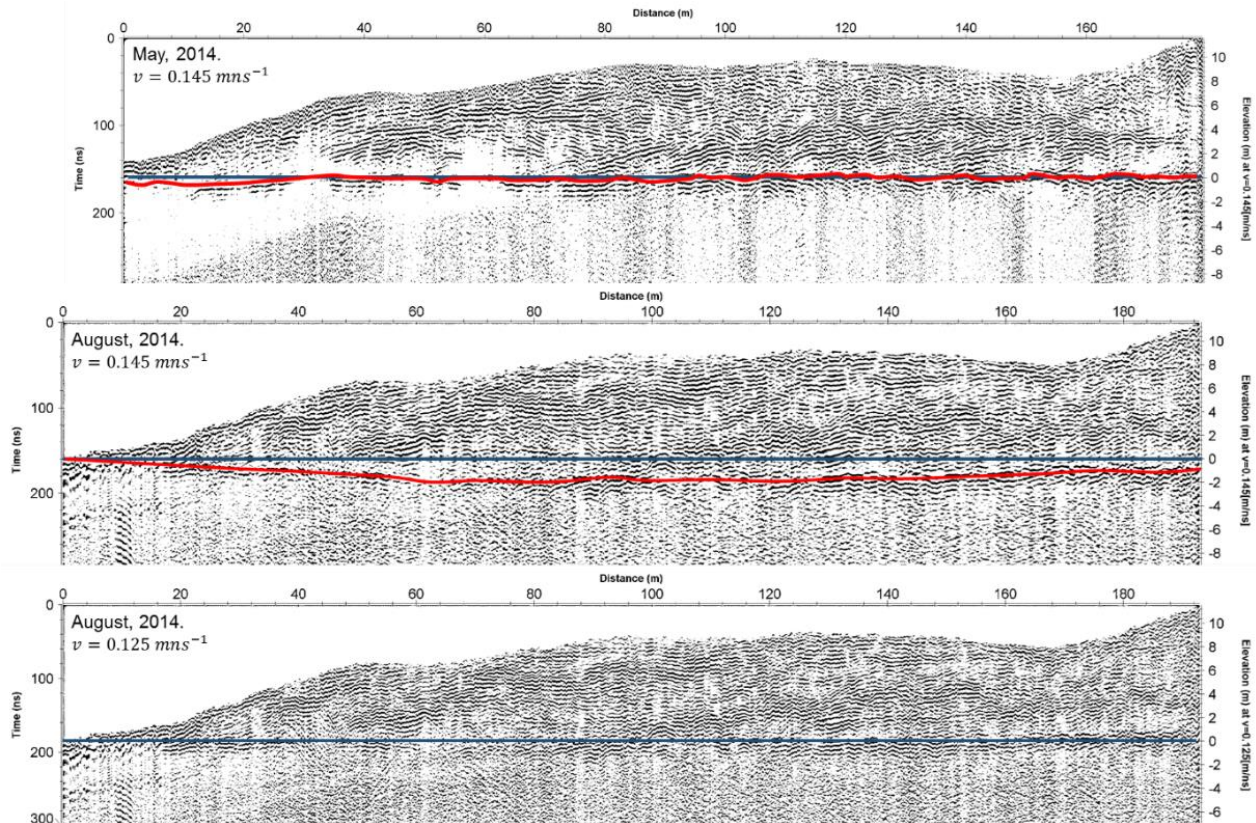


Figure Error! No text of specified style in document..4: Processed GPR data from Line 1a, taken from May (top) and August (middle, bottom). A blue line represents an idealised flat water-table assumption at 0 mASL. The upper and middle sections are migrated with a velocity of 0.145 m/ns, where the August transect violates the flat-water table assumption. The difference in the water-table reflection is an assumed result of water suspended in the zone above the water table, resulting in a slower velocity wave.

Diffraction hyperbola analysis of the August transect suggests a velocity of 0.125 m/ns is the appropriate velocity. We assume the change in velocity is dominantly due to additional water in the immediate subsurface. A 0.02 m/ns velocity change can be linked to an approximately 3.5% increase in the water content within the saturated zone, using the Topp Relationship. As expected, there is an increase in water in the vadose zone in August when compared to May.

Table Error! No text of specified style in document..1: Calculation of the saturation difference via Topp relationship.

| v (m/ns) | ϵ | θ | Θ (%) | $\Delta \Theta$ (%) |
|----------|------------|----------|--------------|---------------------|
| 0.145 | 4.275 | 0.062 | 6.211 | 3.547 |
| 0.125 | 5.752 | 0.098 | 9.758 | |

Figure **Error! No text of specified style in document..5** shows the May transects from the investigation site in 3D. All transects show common features including the water-table, and dune-structures. However limestone spurs are only observed in Line 2 and 4, and correlate with areas of higher topographical relief. A horizontal continuous layer above the water-table can be seen across many of the profiles here. This layer is too high to be the water-table (~2m above sea level), however we speculate this may represent a hydraulically altered layer from periods of higher water table levels, or the capillary fringe.

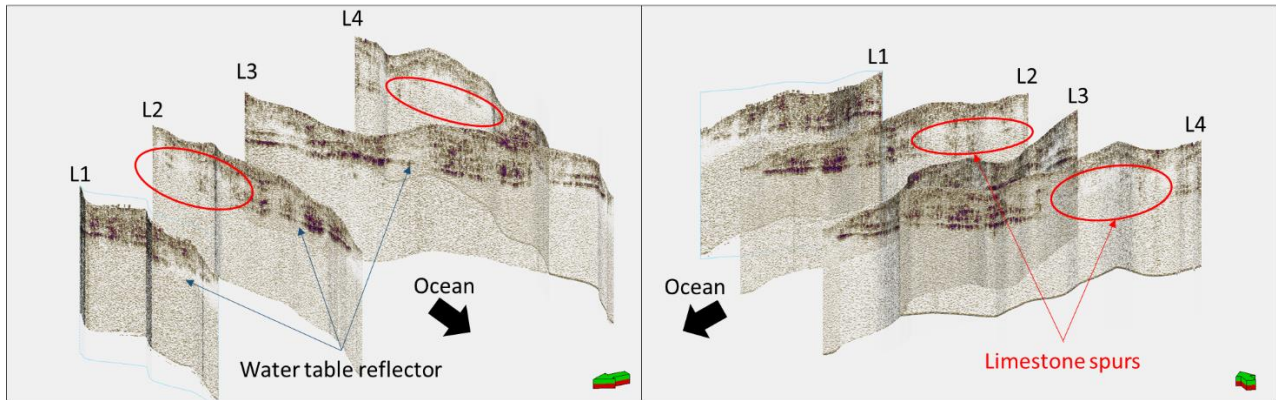


Figure Error! No text of specified style in document..5: Visualisation of GPR data from the investigation site. The water-table reflector is prominently shown, and the limestone spur can be readily identified. Left and right images show the May GPR data from the north and south respectively.

Figure **Error! No text of specified style in document..6** highlights the reflectors identified from the Line 1 transect. A strong water table reflector continuous throughout the profile was readily identified, however no reflectors could be identified below the water table, likely due to a combination of saline water at the coast, and elevation throughout the dunes.

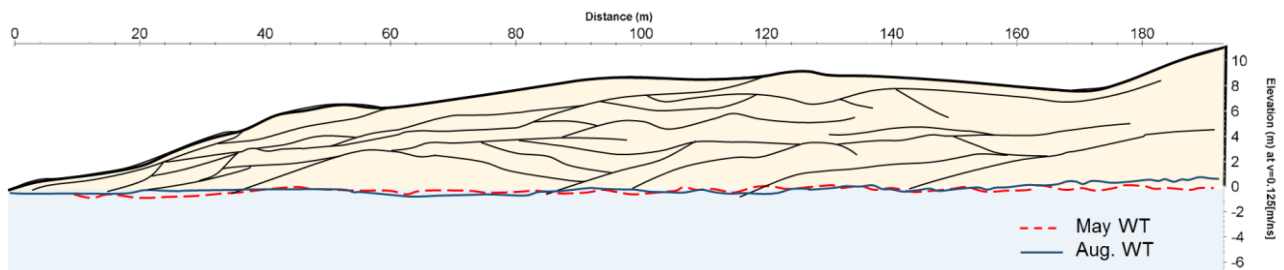


Figure Error! No text of specified style in document..6: Schematic interpretation of GPR reflectors seen in Line 1. May and August water table reflectors are interpreted at the velocities 0.145 m/ns and 0.125 m/ns, showing the flat-water table approximation dependency on volumetric water content in the vadose zone. No sub-water table reflectors were identified.

DISCUSSION

Several assumptions are made throughout this experiment, which include assumptions on the homogeneity of the subsurface, as well as the rate-of-movement through the vadose zone. It is clear that the homogeneity of some sections is incorrect, given the obvious differences in subsurface reflectors across the profile, e.g. limestone spurs, however the section for which the analysis was used (Line 1) is obviously more uniform than other sections, such as Line 2, and Line 4. The water-table is difficult or impossible to resolve in most cases as the limestone appears to have scattered the GPR signal, and so we have based our analysis mostly on line 1, which offers the clearest image of the primary features required for our analysis.

Given the potential rate of infiltration associated with dune sands can be rapid, the long time period between each survey may have resulted in recharge events fully migrating through the vadose zone to the water table. Transition rates in the coarse beach sand will be rapid, however on the built-up vegetated dune faces, the fine-grained wind-borne sediments will naturally decrease this rate. A solution would be to repeat the surveys on a regular, short-period basis, to determine the exact changes present, as well as performing measurements in the laboratory to determine the rate of movement through the sands.

Tidal fluctuations of the order of 0.5 – 1 metres will affect the water table reflector near the coast. The GPR measurements made during this study were at similar tidal levels, however if more regular surveys are planned, the tidal fluctuations must be taken into account.

CONCLUSIONS

We demonstrate that GPR can be effective for time-lapse water infiltration monitoring, showing a decrease in velocity associated with increased volumetric water content in accordance with the Topp relationship. We estimate that, over the time period between measurements, the saturated water volume has increased by approximately 3.5% as inferred by a bulk velocity change of 0.02 m/ns. With the two surveys acquired for this pilot study, we are unable to estimate the physical amount of water in the vadose zone using changes in water-table reflection associated with an increase in vadose-

zone water saturation. However, it can be used to further quantitatively assess groundwater recharge through geophysical measures, and with regular monitoring, the hydraulic parameters of the dune structure could be inferred.

ACKNOWLEDGMENTS

We wish to sincerely thank and acknowledge the work and assistance of Dr. Andrew Greenwood and Dr. Andrew Pethick in the collection of GPR data, and technical advice, and Dr. Elmar Strobach for assistance and valuable commentary on processing and interpretation of the dataset.

REFERENCES

- Allison, G., & Hughes, M. (1978). The use of environmental chloride and tritium to estimate total recharge to an unconfined aquifer. *Soil Research*, 16(2), 181-195.
- Bradford, J. H., Clement, W. P., & Barrash, W. (2009). Estimating porosity with ground-penetrating radar reflection tomography: A controlled 3-D experiment at the Boise Hydrogeophysical Research Site. *Water Resources Research*, 45(4).
- BurVal Working Group, Kirsch, R., Rumpel, H.-M., Scheer, W., & Wiederhold, H. (2006). *Groundwater resources in buried valleys: a challenge for geosciences*: Leibniz Institute for Applied Geosciences (GGA-Institut).
- Butler, D. K. (2005). *Near-surface geophysics*: Society of Exploration Geophysicists Tulsa.
- Buynevich, I. V., Jol, H. M., & FitzGerald, D. M. (2009). Chapter 10 - Coastal Environments. In *Ground Penetrating Radar Theory and Applications* (pp. 299-322). Amsterdam: Elsevier.
- Davis, J. L., & Annan, A. P. (1989). Ground-Penetrating Radar for High-Resolution Mapping of Soil and Rock Stratigraphy. *Geophysical Prospecting*, 37(5), 531-551. doi:10.1111/j.1365-2478.1989.tb02221.x
- Huisman, J. A., Hubbard, S. S., Redman, J. D., & Annan, A. P. (2003). Measuring Soil Water Content with Ground Penetrating Radar: A Review. *Vadose Zone Journal*, 2(4), 476-491. doi:10.2136/vzj2003.4760
- Sharma, M., Farrington, P., & Fernie, M. (1983). *Localized groundwater recharge on the "Gnangara Mound", Western Australia*. Paper presented at the international conference on groundwater and man.
- Stephens, D. B., & Knowlton, R. (1986). Soil water movement and recharge through sand at a semiarid site in New Mexico. *Water Resources Research*, 22(6), 881-889.
- Strobach, E. (2013). Hydrogeophysical investigation of water recharge into the Gnangara Mound.
- Strobach, E., D. Harris, B., Christian Dupuis, J., W. Kopic, A., & W. Martin, M. (2010). Ground-Penetrating Radar For Delineation Of Hydraulically Significant Layers In The Unsaturated Zone Of The Gnangara Mound, Wa. *ASEG Extended Abstracts*, 2010(1), 1-4. doi:<http://dx.doi.org/10.1071/ASEG2010ab237>
- Strobach, E., Harris, B. D., Dupuis, J. C., & Kopic, A. W. (2014). Time-lapse borehole radar for monitoring rainfall infiltration through podosol horizons in a sandy vadose zone. *Water Resources Research*, 50(3), 2140-2163. doi:10.1002/2013wr014331
- Topp, G. C., Davis, J. L., & Annan, A. P. (1980). Electromagnetic Determination of Soil-Water Content - Measurements in Coaxial Transmission-Lines. *Water Resources Research*, 16(3), 574-582. doi:DOI 10.1029/WR016i003p00574
- Turesson, A. (2006). Water content and porosity estimated from ground-penetrating radar and resistivity. *Journal of Applied Geophysics*, 58(2), 99-111. doi:10.1016/j.jappgeo.2005.04.004